EXTRACTING EFFECTIVE FEATURES FROM HIGH DENSITY NIRS-BASED BCI FOR ASSESSING NUMERICAL COGNITION

Kai Keng Ang, Juanhong Yu, Cuntai Guan

Institute for Infocomm Research – Agency for Science and Technology And Research, Singapore
Email: {kkang, jyu, ctguan}@i2r.a-star.edu.sg

ABSTRACT

Near-infrared spectroscopy (NIRS)–based Brain-Computer Interface (BCI) was recently proposed to assess level of numerical cognition in subjects. However, existing feature extraction method was only proposed for low density 16 channels NIRS-based BCI. This study investigates the performance of a high density 348 channels NIRS-based BCI on 8 healthy subjects while they solve mental arithmetic problems with two difficulty levels and the rest condition. A novel method of extracting effective features from high density single-trial NIRS data is proposed using common average reference spatial filtering and single-trial baseline reference. The performance of the proposed feature extraction method is presented using 5×5-fold cross-validations on the single-trial NIRS data collected using mutual information-based feature selection and support vector machine classifier. The results yielded an overall average accuracy of 73% and 92% in classifying hard versus easy tasks and hard versus rest tasks respectively using the proposed method, compared to 46% and 62% respectively using existing method. The results demonstrated the effectiveness of using the proposed method in high density NIRS-based BCI for assessing numerical cognition.

Index Terms**—** Brain-computer interface, near-infrared spectroscopy, mental arithmetic, feature extraction.

1. INTRODUCTION

Brain-Computer Interface (BCI) is a communication system that directly translates brain signals into commands for external devices [1]. Brain signals can be measured using electroencephalography (EEG), functional magnetic resonance imaging (fMRI), magnetoencephalography (MEG), positron emission tomography (PET), and invasive methods such as electrocorticogram (ECoG) and implanted electrodes [1]. Besides the widespread use of EEG-based BCI for left and right-hand motor imagery, the feasibility of using NIRS-based BCI has also been demonstrated [2], [3].

NIRS is a non-invasive optical neural imaging technique that measures concentration changes of oxyhemoglobin (HbO_2) and deoxyhemoglobin (Hb) in the cerebral vessels by means of different absorption spectra in the near-infrared range [4]. Besides the use of non-invasive NIRS-based BCI for motor imagery, studies have also shown that other cognitive tasks, such as performing mental arithmetic, generally cause an increase of oxyhemoglobin associated with decreases of deoxyhemoglobin in the prefrontal cortex [5]. Recently, the feasibility of using a low density 16 channels non-invasive NIRS-based BCI for assessing level of numerical cognition had been demonstrated in [6], of which has the potential application to investigate how to best teach mathematics in a classroom setting.

The previous study in [6] collected NIRS data from 20 healthy subjects in performing 3 difficulty levels of mental arithmetic tasks. A total of 75 trials of mental arithmetic tasks were collected from each subject, and these trials were evenly distributed into the 3 difficulty levels. The subjects performed two 1-digit additions for the easy tasks, 1-digit and 2-digits additions for the medium tasks, and two 2-digits additions for the hard tasks. However, the data were collected such that 5 trials of the same difficulty level formed a block, and a total of 15 randomized blocks were collected from each subjects. This experiment protocol was designed in blocks of 5 trials in consideration of the slow hemodynamic responses, but inherently included correlated single-trials in each block that comprised of tasks with same difficulty level. The previous study also proposed a simple method of extracting the features by taking the averaged changes in oxyhemoglobin and deoxyhemoglobin across 12 s of NIRS data recorded for a single trial, and results were presented using 5×5-fold cross-validations on the 75 single-trials of NIRS data collected.

This paper presents a study of high density NIRS-based BCI for assessing the level of numerical cognition from performing mental arithmetic tasks. The motivations behind conducting this study compared to the previous study in [6] are: Firstly, to address the correlated single-trials of mental arithmetic tasks executed in blocks of 5 trials in the previous study. Secondly, to investigate the effectiveness of a high density NIRS-based BCI for assessing numerical cognition compared to low density NIRS-based BCI in the previous study. Thirdly, to investigate the effectiveness using the simple feature extraction method from the previous study in a high density NIRS-based BCI. Last but not least, to investigate and propose novel feature extraction methods to improve the performance for high density NIRS-based BCI.

2. METHOD

This section describes the data collection using a high density NIRS-based BCI for assessing numerical cognition, the computation of the hemodynamic responses from the data, the feature extraction method used in the previous study [6], and the proposed feature extraction method.

2.1. NIRS data collection

The data was collected from 8 healthy subjects (3 females, mean age 28.6±8.38) recruited from staffs and students of the Brain Computer Interface laboratory in the Institute for Infocomm Research, A*STAR. All subjects were fully informed, and consented to participate in the study.

The NIRS data was collected using the DYnamic Near-Infrared Optical Tomography (DYNOT) Imaging System (NIRx Medizintechnik GmbH, Berlin, Germany) with two wavelengths (λ = 760 & 830 nm) using 32 optodes that comprised co-located optical fibers, each serving as source and detector, on the prefrontal cortex of the subject's head as shown in Fig. 1(a). The optical fibers were fixed on the prefrontal cortex using an open scaffolding structure with individually spring-loaded fibers to ensure stable optical contact. The setup measured 32 channels from 32 detectors for each source for each wavelength, and this dense fiber grid setup yielded a total of 1024 channels for each wavelength. However, not all channels contained useful data. Thus, only useful channels with source and detector distances between 1.5 to 3.5 cm measured using the Xensor digitizer were used, yielding a total of 348 data channels for each wavelength.

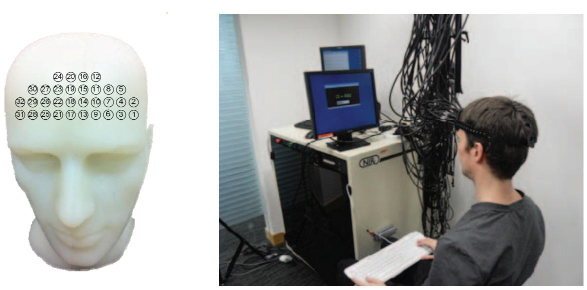

(a) (b)

Fig. 1. (a) Absorption changes are measured using a fiber grid with 32 co-located source and detectors over the prefrontal cortex. (b) NIRS data collection setup whereby the numerical arithmetic question is presented to the subject on the screen and the answer is captured using a keyboard.

2.2. Experimental Protocol

During the data collection, the subjects were seated in a comfortable chair in a room with normal lighting. They were asked to relax before the data collection. They were also asked to minimize movement and to respond as quickly and as correctly as possible during data collection.

The subjects underwent a total of 40 trials of mental arithmetic tasks that were evenly distributed into 2 difficulty levels of easy and hard. Each trial comprised of 3 numerical arithmetic questions from the same difficulty level. The subjects performed mental additions of 3-digits number with 2-digits number without carryover for the easy tasks (eg. 543 + 12), and additions of 4-digits numbers with 3-digits with at least 1 carry over (eg. 5432 + 612) for the hard tasks. At the start of each trial, a question was displayed for a maximum of 12 s. The next question will be displayed immediately if the subject responded within 12 s, or at the end of 12 s. A period of 20 s of rest condition was given between each trial. If all the 3 questions from a trial were correctly answered, then the trial was considered correct.

2.3. NIRS data preprocessing

Let the optical density for wavelength λ from a source and detector channel c be denoted as OD_c^λ. First, the normalized change in optical density $\Delta\overline{\mathrm{OD}}_c^\lambda$ was computed by dividing each time sample with the mean of the optical signal acquired for the entire session. Next, $\Delta\overline{\mathrm{OD}}_c^\lambda$ was low-pass filtered using Chebychev type II filter with a cut-off frequency of 0.14 Hz and pass-band attenuation of 0.02 dB. Subsequently, linear-detrending was performed to remove the drift (low frequency bias) in the NIRS data due to reasons, such as subject movement, blood pressure variation, and instrumental instability [7]. After filtering and detrending, unity was added to bring the mean of the optical density to unity instead of zero. The optical density changes were represented as $\Delta\mathrm{OD}_c^\lambda$ after these preprocessing steps.

2.4. Computing hemodynamic responses

The optical density changes $\Delta\mathrm{OD}_c$ were expressed as a linear combination of the changes in oxyhemoglobin $\Delta[\mathrm{HbO_2}]_c$ and deoxyhemoglobin $\Delta[\mathrm{Hb}]_c$ using the modified Beer-Lambert law (MBLL) [8], [9] given by

$$\Delta\mathrm{OD}_c^\lambda = L^\lambda \mathrm{DPF}^\lambda \left(\varepsilon_{\mathrm{Hb}}^\lambda \Delta\left[\mathrm{Hb}\right]_c + \varepsilon_{\mathrm{HbO_2}}^\lambda \Delta\left[\mathrm{HbO_2}\right]_c\right), \quad (1)$$

where ε^λ is the wavelength-dependent extinction coefficient, L^λ is the path length from source to detector, and DPF^λ is the differential path-length. In this study, the values of ε^λ are obtained from [10], and DPF^λ = 6.3 and 6.0 are used for λ = 760 and 830 nm respectively.

The optical density changes from the two wavelength were converted to changes in $\mathrm{HbO_2}$ and HB by solving [2]

$$\begin{bmatrix} \Delta\left[\mathrm{HbO_2}\right]_c \\ \Delta\left[\mathrm{Hb}\right]_c \end{bmatrix} = \left(\mathbf{E}^T\mathbf{E}\right)^{-1}\mathbf{E}^T \begin{bmatrix} \Delta\mathrm{OD}_c^{\lambda_1} / L^{\lambda_1}\mathrm{DPF}^{\lambda_1} \\ \Delta\mathrm{OD}_c^{\lambda_2} / L^{\lambda_2}\mathrm{DPF}^{\lambda_2} \end{bmatrix}, \quad (2)$$

where

$$\mathbf{E} = \begin{bmatrix} \varepsilon_{HbO_2}^{\lambda_1} & \varepsilon_{Hb}^{\lambda_1} \\ \varepsilon_{HbO_2}^{\lambda_2} & \varepsilon_{Hb}^{\lambda_2} \end{bmatrix}. \quad (3)$$

2.5. Feature extraction method in previous study

The feature extraction method in the previous study [6] was performed by taking the average $\Delta[\mathrm{HBO_2}]_c$ across a time segment T of NIRS data recorded for a single trial given by

$$\Delta\left[\mathrm{HbO_2}\right]_c = \frac{1}{T}\int_0^T \Delta\left[\mathrm{HbO_2}\right]_c(t), \quad (4)$$

and the average of $\Delta[\mathrm{HB}]_c$ can be similarly performed. The extracted feature vector for the i^{th} trial was then formed using

$$\mathbf{x}_i = \left[\Delta\left[\mathrm{HbO_2}\right]_1 \cdots \Delta\left[\mathrm{HbO_2}\right]_{n_c} \quad \Delta\left[\mathrm{Hb}\right]_1 \cdots \Delta\left[\mathrm{Hb}\right]_{n_c}\right], \quad (5)$$

where $\mathbf{x}_i \in \mathbb{R}^{1\times n_t}$, i=1,2,…,n_t; n_t denotes the total number of trials in the training data, and n_c denotes the total number of channels for each wavelength.

The feature matrix for the training data was then formed by $\mathbf{X} = \left[\mathbf{x}_1 \quad \mathbf{x}_2 \quad \cdots \quad \mathbf{x}_{n_t}\right]^T$.

2.6. Proposed feature extraction method

NIRS signals are often dominated by noise and artifacts of both physical and physiological origin, such as subject's movement, heartbeat, respiration effects and other trends [11]. The filtering and detrending performed in section 2.3 might not be sufficient to remove all the noise and artifacts. Therefore, the Common Average Reference (CAR) Spatial Filtering, commonly used in EEG-based BCI [12], is proposed to reduce noise and artifacts that are common in all the channels. The CAR method was performed on $\Delta[\mathrm{HBO_2}]_c$ using

$$\Delta\overline{\left[\mathrm{HbO_2}\right]}_c(t) = \Delta\left[\mathrm{HbO_2}\right]_c(t) - \frac{1}{n_c}\sum_{j=1}^{n_c}\Delta\left[\mathrm{HbO_2}\right]_c(t), \quad (6)$$

and CAR was similarly performed on $\Delta[\mathrm{HB}]_c$.

After performing CAR, Single-trial Baseline Reference (SBR) is proposed to reduce noise and artifacts in each specific channel. The SBR method was performed on $\Delta[\mathrm{HBO_2}]_c$ using

$$\Delta\left[\mathrm{HbO_2}\right]_c = \frac{2}{T}\left(\int_{T/2}^{T}\Delta\overline{\left[\mathrm{HbO_2}\right]}_c(t) - \int_0^{T/2}\Delta\overline{\left[\mathrm{HbO_2}\right]}_c(t)\right), \quad (7)$$

and SBR on $\Delta[\mathrm{HB}]_c$ was similarly performed. The proposed SBR method first computes the baseline reference for a single trial from the average of the first half of the time segment T, then subtracts this baseline reference from the next half of the time segment for $\Delta[\mathrm{HBO_2}]_c$ and $\Delta[\mathrm{HB}]_c$ respectively. The extracted feature vector for the i^{th} trial is then formed using equation (4) whereby $\Delta[\mathrm{HBO_2}]_c$ and $\Delta[\mathrm{HB}]_c$ are computed from equation (7).

2.7. Feature selection and classification

Feature selection was then performed to select discriminative features using the Mutual Information-based Best Individual Feature (MIBIF) algorithm [13] on the training data. In this study, the MIBIF algorithm was used to select 10 features, and the Support Vector Machine (SVM) was used to classify the selected features.

3. EXPERIMENTAL RESULTS

The performance of the NIRS-based BCI was then evaluated using 5×5-fold cross-validations in classifying the single-trial high density NIRS data on easy versus hard (EvH) tasks, easy versus rest (EvR) tasks, and hard versus rest (HvR) tasks. The time segment T for classifying the EvH tasks was computed for each subject based on the average time taken to answer all the 3 arithmetic questions in a single trial. The time segment of a fixed T=14 s was used for classifying EvR and HvR tasks.

Table 1. Experimental results on the number of correct trials answered by the subjects, 5×5-fold cross-validations accuracies and standard deviations in classifying the single-trial high density NIRS data on Easy versus Hard (EvH), Easy versus Rest (EvR), and Hard versus Rest (HvR) tasks using MIBIF to select 10 out of 686 extracted features and Support Vector Machine classifier. The classification accuracies are obtained on features extracted using: method in [6], single-trial baseline reference (SBR), and SBR after common average reference spatial filter (CAR-SBR)

	Correct	Method in [6]			SBR method			CAR-SBR method		
Subjects	Trials	EvH	EvR	HvR	EvH	EvR	HvR	EvH	EvR	HvR
1	32	34.0 ± 4.9	37.0 ± 7.4	39.5 ± 4.8	55.0 ± 4.0	67.5 ± 5.9	67.5 ± 4.3	59.5 ± 4.5	59.5 ± 3.7	84.0 ± 3.4
2	23	55.0 ± 4.0	64.5 ± 4.8	71.0 ± 5.2	79.0 ± 4.5	84.0 ± 2.9	92.0 ± 3.3	71.0 ± 7.2	97.5 ± 3.1	95.0 ± 2.5
3	28	60.0 ± 8.8	84.5 ± 2.7	82.0 ± 2.7	76.0 ± 6.8	97.0 ± 1.1	96.0 ± 1.4	74.0 ± 2.9	100 ± 0.0	96.0 ± 1.4
4	33	57.5 ± 6.4	45.0 ± 5.3	78.5 ± 7.6	70.5 ± 5.4	76.5 ± 3.8	96.5 ± 2.9	73.5 ± 7.4	80.5 ± 3.3	97.0 ± 1.1
5	24	36.0 ± 8.4	45.0 ± 2.5	54.0 ± 4.2	64.0 ± 6.8	71.5 ± 2.9	91.5 ± 2.2	78.5 ± 2.9	59.5 ± 8.9	84.0 ± 5.8
6	30	32.0 ± 3.3	34.0 ± 6.8	42.0 ± 6.0	62.0 ± 7.8	65.0 ± 8.3	89.0 ± 2.9	72.0 ± 7.6	61.0 ± 7.4	96.0 ± 2.2
7	35	44.5 ± 2.7	41.5 ± 5.5	69.0 ± 3.4	59.0 ± 8.4	75.0 ± 4.0	80.5 ± 3.3	61.0 ± 1.4	74.0 ± 4.5	85.5 ± 3.3
8	31	50.0 ± 7.7	37.0 ± 8.0	61.5 ± 6.8	89.5 ± 2.1	86.5 ± 2.2	100 ± 0.0	91.5 ± 2.2	83.5 ± 5.2	100 ± 0.0
Average		46.1 ± 5.8	48.6 ± 5.4	62.2 ± 5.1	69.4 ± 5.7	77.9 ± 3.9	89.1 ± 2.5	72.6 ± 4.5	76.9 ± 4.5	92.2 ± 2.4

Table 1 shows the number of trials whereby all 3 questions were correctly answered by the subjects, and the classification accuracies obtained on the features extracted using: method in [6], SBR method described in section 2.6, and proposed CAR-SBR method described in section 2.6. The results showed that the classification of the EvH tasks using the feature extraction method in [6] yielded an averaged accuracy of 46.1% across the 8 subjects. This random chance level accuracy is in contrast with the result of 69.8% presented in [6]. The reasons are twofold: Firstly, the study in [6] was performed on 16 channel low density NIRS-based BCI. Thus this showed that the feature extraction method in [6] was not effective in high density NIRS-based BCI for mental arithmetic task. Secondly, the result in [6] was better because the previous experiment was performed in a block of 5 trials on the same difficulty level. Thus this showed that the NIRS data from trials in the same block in [6] were correlated.

The results in Table 1 also showed that the classification of EvH tasks on features extracted using the SBR and CAR-SBR methods yielded significantly improved averaged accuracies of 69.4% and 72.6% compared to 46.1% using the method in [6] (p=0.0002, 0.0006 using paired t-test respectively). Although the results on the CAR-SBR method was not significantly different from the SBR method (p=0.223), the former yielded an improvement of 3.3% over the latter. Furthermore, the results on the classification of the HvR tasks and the EvR tasks on features extracted using the proposed CAR-SBR method showed significantly improved averaged accuracies of 92.2% and 76.9% compared to 62.2% and 48.6% respectively using the method in [6] (p=0.0006, 0.0001). The results on classifying the HvR tasks was also significantly better than classifying the EvR tasks (p=0.0149). This showed that the NIRS data of the subjects performing harder mental arithmetic tasks are more separated from the NIRS data at rest condition compared to the easier mental arithmetic tasks. In addition, the results also showed that the accuracies of classifying the EvH and HvR tasks using the proposed CAR-SBR method were not correlated to the number of correctly answered trials by the subjects (r=-0.30, -0.03).

4. CONCLUSIONS

This paper presents a novel method of extracting effective features from high density NIRS-based BCI using common average reference spatial filtering and single-trial baseline reference. A study was performed to collect a dense 348 channels of NIRS data for each wavelength from the prefrontal cortex of 8 subjects in performing two difficulty levels of mental arithmetic and the rest condition.

The results showed that existing method for low density NIRS-based BCI was not effective in the high density NIRS-based BCI, and the results presented in the previous study may be a result of correlated trials executed in a block. The results in this study showed that the proposed method yielded significantly improved classification accuracies compared to existing method. Furthermore, the results also revealed no correlation between the classification accuracies and the number of correctly answered trials. Hence the results demonstrated the effectiveness of using the proposed method in high density NIRS-based BCI for mental arithmetic task, as well as the application of such a BCI to provide a feedback on the level of numerical cognition.

5. REFERENCES

[1] J. R. Wolpaw, N. Birbaumer, D. J. McFarland, G. Pfurtscheller, and T. M. Vaughan, "Brain-computer interfaces for communication and control," *Clin. Neurophysiol.,* vol. 113, no. 6, pp. 767-791, Jun. 2002.

[2] R. Sitaram, H. Zhang, C. Guan, M. Thulasidas, Y. Hoshi, A. Ishikawa, K. Shimizu, and N. Birbaumer, "Temporal classification of multichannel near-infrared spectroscopy signals of motor imagery for developing a brain-computer interface," *NeuroImage,* vol. 34, no. 4, pp. 1416-1427, Feb. 2007.

[3] S. M. Coyle, T. E. Ward, and C. Markham, M., "Brain-computer interface using a simplified functional near-infrared spectroscopy system," *J. Neural Eng.,* vol. 4, no. 3, p. 219, Sep. 2007.

[4] A. Villringer and B. Chance, "Non-invasive optical spectroscopy and imaging of human brain function," *Trends in Neurosciences,* vol. 20, no. 10, pp. 435-442, 1997.

[5] M. Tanida, K. Sakatani, R. Takano, and K. Tagai, "Relation between asymmetry of prefrontal cortex activities and the autonomic nervous system during a mental arithmetic task: near infrared spectroscopy study," *Neurosci. Lett.,* vol. 369, no. 1, pp. 69-74, 2004.

[6] K. K. Ang, C. Guan, K. Lee, J. Q. Lee, S. Nioka, and B. Chance, "A Brain-Computer Interface for Mental Arithmetic Task from Single-Trial Near-Infrared Spectroscopy Brain Signals," in *Proc. 20th Int. Conf. on Pattern Recogn.*, 2010, pp. 3764-3767.

[7] N. Thakor, "In the Spotlight: Neuroengineering," *IEEE Reviews in Biomedical Engineering,* vol. 2, pp. 18-20, 2009.

[8] R. Leeb, F. Lee, C. Keinrath, R. Scherer, H. Bischof, and G. Pfurtscheller, "Brain-Computer Communication: Motivation, Aim, and Impact of Exploring a Virtual Apartment," *IEEE Trans. Neural Syst. Rehabil. Eng.,* vol. 15, no. 4, pp. 473-482, Dec. 2007.

[9] A. Kubler, V. K. Mushahwar, L. R. Hochberg, and J. P. Donoghue, "BCI meeting 2005-workshop on clinical issues and applications," *IEEE Trans. Neural Syst. Rehabil. Eng.,* vol. 14, no. 2, pp. 131-134, Jun 2006.

[10] M. Cope, "The application of near infrared spectroscopy to non invasive monitoring of cerebral oxygenation in the newborn infant, Ph.D Thesis," University College London, London, 1991.

[11] F. Matthews, B. A. Pearlmutter, T. E. Ward, C. Soraghan, and C. Markham, "Hemodynamics for Brain-Computer Interfaces," *IEEE Signal Process. Mag.,* vol. 25, no. 1, pp. 87-94, 2008.

[12] Y. Li, K. K. Ang, and C. Guan, "Digital Signal Processing and Machine Learning," in *Brain-Computer Interfaces: Revolutionizing Human-Computer Interaction*. B. Graimann, B. Allison, and G. Pfurtscheller, Eds. Berlin: Springer, 2011, pp. 305-330.

[13] K. K. Ang, Z. Y. Chin, H. Zhang, and C. Guan, "Mutual information-based selection of optimal spatial-temporal patterns for single-trial EEG-based BCIs," *Pattern Recogn.,* vol. In Press, Accepted Manuscript, 2012.